SAND77-8300
Unlimited Release

The Effectiveness of Spectrally Selective Surfaces for Exposed, High-Temperature Solar Absorbers

M. Abrams

Prepared by Sandia Laboratories, Albuquerque, New Mexico 87115 and Livermore, California 94550 for the United States Department of Energy under Contract AT (29-1)-789.

Printed January 1978

Sandia Laboratories
energy report

When printing a copy of any digitized SAND Report, you are required to update the markings to current standards.

SF 2900-QQB(3-74)

Issued by Sandia Laboratories, operated for the United States Department of Energy by Sandia Corporation.

NOTICE

This report was prepared as an account of work sponsored by the United States Government. Neither the United States nor the United States Department of Energy, nor any of their employees, nor any of their contractors, subcontractors, or their employees, makes any warranty, express or implied, or assumes any legal liability or responsibility for the accuracy, completeness or usefulness of any information, apparatus, product or process disclosed, or represents that its use would not infringe privately owned rights.

SAND77-8300
Unlimited Release
Printed January 1978

THE EFFECTIVENESS OF SPECTRALLY SELECTIVE SURFACES FOR EXPOSED, HIGH-TEMPERATURE SOLAR ABSORBERS

M. Abrams
Thermal Sciences Division 8124
Sandia Laboratories
Livermore, California 94550

ABSTRACT

A theoretical heat transfer analysis of spectrally selective absorbers showed that spectral selectivity offers the greatest benefits for conditions of high absorber temperature and/or low values of solar irradiation. By using a two-band model of the selective absorber, it was found that the cutoff wavelength which maximizes absorber efficiency depends on just two parameters: the absorber temperature, and the level of solar irradiation. The emittance of the infrared band was found to have a greater effect upon efficiency than the absorptance of the solar band when a critical dimensionless parameter exceeds unity.

NOMENCLATURE

C_1, C_2	Planck radiation constants $C_1 = 5.9544 \times 10^{-13}$ W-cm^2 $C_2 = 14388 \mu m$-°K
$e_{b\lambda}(T)$	spectral emissive power of black surface at absolute temperature T
$F_{emit,\lambda_c}(T)$	fraction defined by Equation (7)
F_{sol,λ_c}	fraction defined by Equation (6)
G_{sol}	total solar irradiation normal to absorber surface (MW/m^2)
$G_{sol,\lambda}$	spectral solar irradiation normal to absorber surface (MW/m^2-μm)
I	percent improvement attainable by using a spectrally selective surface instead of a non-selective (or gray) surface
Q_{abs}	rate of energy absorption (MW/m^2)
Q_{emit}	rate of thermal emission (MW/m^2)
T	absolute temperature of absorber surface (°K)
T_s	temperature of absorber surface (°F)
T_{sol}	temperature of black surface whose spectral emissive power is assumed to characterize air mass 0 solar irradiation
x	dimensionless parameter $C_2/\lambda_c T$
α_1, α_2	respectively, high and low absorptances in two-band model of spectrally selective surface (Figure 1)

α_λ	spectral hemispherical absorptance
α	total hemispherical absorptance
ε_λ	spectral hemispherical emittance
ε	total hemispherical emittance
η	absorber efficiency (Equation (1))
η_{max}	efficiency of selective surface with optimum cutoff wavelength
$\eta_{non-selective}$	efficiency of non-selective (gray) surface
λ	wavelength of radiation (μm)
λ_c	cutoff wavelength (μm)
$\lambda_{c,max}$	cutoff wavelength which maximizes efficiency of absorber (μm)
σ	Stefan-Boltzmann constant 5.6693×10^{-14} MW/m^2-K^4

Introduction

In several solar power plant concepts, the solar energy reflected from a large field of mirrors is focussed onto a high-temperature, convex, absorber surface which is exposed to the environment. The 10 and 100 megawatt power plants proposed by the McDonnell-Douglas Company are examples [1]. In contrast to cavity-type absorbers of solar energy, all of the energy that would be reflected and thermally emitted from such exposed surfaces is lost and cannot be recaptured.

A heat transfer analysis of exposed absorbers was, therefore, undertaken to determine whether making them spectrally selective would substantially increase their effectiveness by simultaneously maximizing the absorption of solar energy and minimizing the emission of infrared. The analysis employs a two-band model of the spectrally selective surface: a high absorptance is assumed up to a given cutoff wavelength λ_c (beneath which most of the solar spectrum lies), and then, a low absorptance is assumed for the remainder of the spectrum (Figure 1). Since, at a given wavelength, emittance equals absorptance, infrared emission beyond λ_c is suppressed.

A variety of techniques exist which can produce, approximately, spectral selectivity in a metal. Peterson and Ramsey [2] mention several:

(i) coating the metal with a layer of material (a semi-conductor) having a high absorption coefficient for solar energy, but having transparency to the infrared; this allows the low emittance characteristics of the metal to "show" through;

(ii) depositing a layer of transparent material to a thickness (~1000 Å) such that light reflected from the metal interferes destructively with light reflected from the front surface of the coating; the coating is sufficiently thin so that the low infrared emittance of the metal is preserved;

(iii) introducing pores having a size distribution such that the metallic surface appears rough (and, therefore, highly absorbing) to solar radiation, but smooth to the longer wavelength infrared.

Special paints and electroplated coatings have also been found to produce some degree of spectral selectivity [3]. The analysis employed here, however, is independent of these techniques.

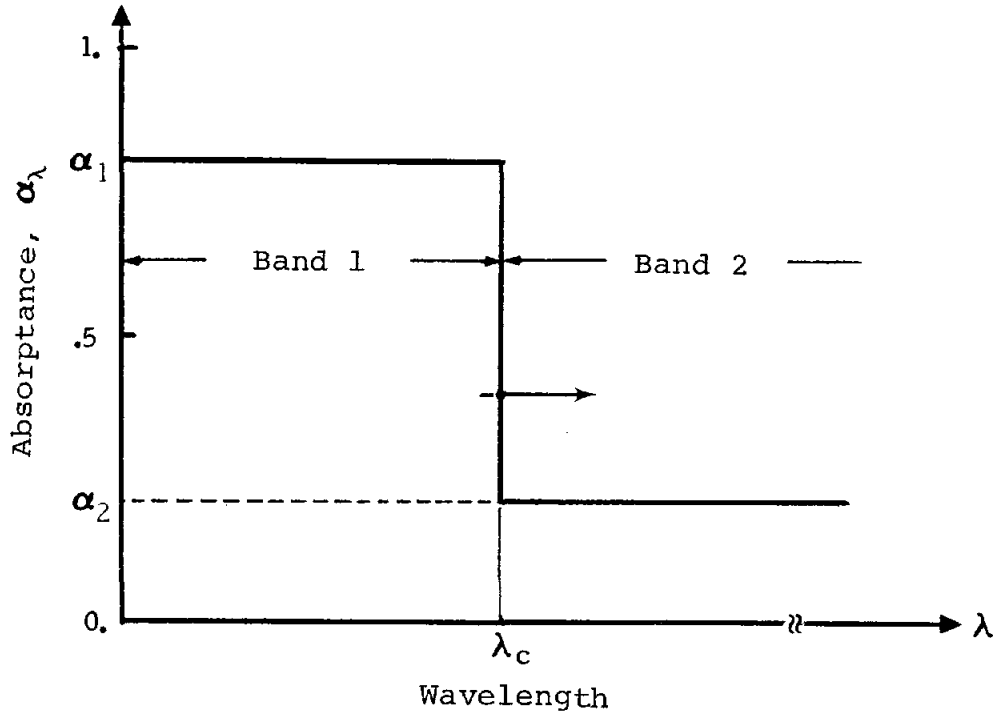

Figure 1. Absorptance model of two-band spectrally selective surface.

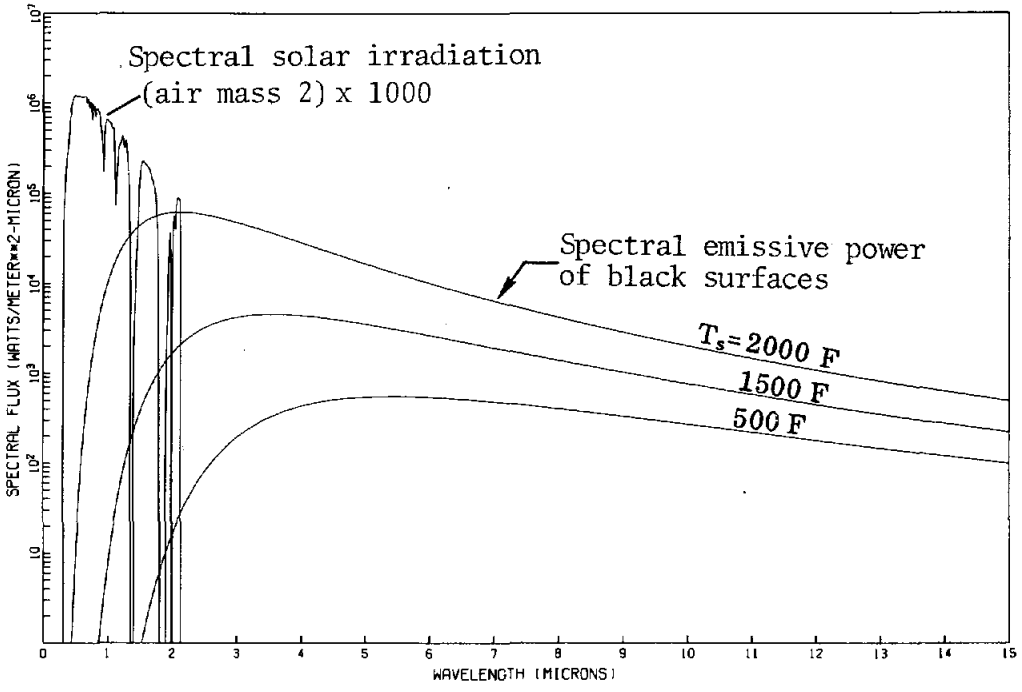

Figure 2. Comparison of solar and infrared spectra. Solar irradiation after Moon [6, page 16-9].

The present study has three objectives:

(a) quantifying the improvement in performance attainable by using a spectrally selective surface instead of one merely having a constant value of the absorptance over the entire spectrum;

(b) determining the sensitivity of performance to the absorptances of each band;

(c) determining the cutoff wavelength at which the transition from high to low absorptance should occur in order that the improvement in performance be maximized.

The latter objective is not necessarily trivial, since at elevated temperatures, there is no clear boundary between the solar and infrared spectra. Figure 2 shows this.

No attempt is made to supplant heat transfer calculations that account for the details of the absorptance spectrum of a real surface, and convective and conductive losses. Rather, the intent is to provide guidance to the systems engineer who would want to know whether selective coatings are worth considering in a given application; and to the material scientist who may want to know the effects upon performance of altering a cutoff wavelength or the band absorptances.

Summary

Absorber performance is quantified by an efficiency

$$\eta \equiv \frac{\text{Absorbed solar energy - Emitted thermal energy}}{\text{Incident solar energy}}$$

Efficiency, thus defined, is a direct measure of the net amount of energy input to an absorber. A mathematical expression for efficiency was obtained in terms of the variables: solar irradiation, absorber temperature, the band absorptances, and the cutoff wavelength.

By using this expression it was found that it becomes increasingly advantageous to employ a spectrally selective surface as the absorber temperature increases and/or the solar irradiation decreases.

The cutoff wavelength maximizing efficiency was found to depend upon just two parameters: the solar irradiation, and the absorber temperature. It becomes increasingly important that the cutoff wavelength be near the optimum value for high absorber temperature and low-level irradiation.

The efficiency was found to be more sensitive to the solar (band 1) absorptance than the infrared (band 2) absorptance when the dimensionless parameter $\sigma T^4/G_{sol}$ is less than unity. However, the reverse was found to be true when this parameter exceeds unity.

Analysis

The performance of an absorber is quantified by an efficiency defined as

$$\eta \equiv \frac{\text{Absorbed solar energy - Emitted thermal energy}}{\text{Incident solar energy}}$$

or

$$\eta \equiv \frac{Q_{abs} - Q_{emit}}{G_{sol}} \qquad (1)$$

A surface that absorbed all the incident solar energy and emitted no thermal energy would have an efficiency of 1*; while a surface whose temperature level were such that emission exceeded absorption would have a negative efficiency. Expressions for efficiency are developed below for three cases:

a. the surface has the absorptance characteristics depicted in Figure 1;

b. the surface is non-selective with the absorptance of band 1 over the entire spectrum (i.e., the surface is gray);

c. the actual spectral dependence of α_λ is unspecified, but total hemispherical emittance and absorptance data embodying this dependence are known.

*Efficiency would be 1 in the case of a black absorber at 0 degrees absolute.

Another frequently-used measure of absorber performance is simply the ratio α/ε where α and ε are, respectively, the total hemispherical absorptance and emittance of the surface. It is shown later, however, that this ratio, by itself, may not be a reliable indicator of the net amount of energy transferred into the absorber surface; whereas the efficiency defined by Equation (1) is.

a. Efficiency of the two-band spectrally selective surface (Figure 1)

The absorbed solar energy may be expressed as the sum of the energies absorbed in bands 1 and 2, i.e.,

$$Q_{abs} = \int_0^{\lambda_c} \alpha_\lambda \, G_{sol,\lambda} \, d\lambda + \int_{\lambda_c}^{\infty} \alpha_\lambda \, G_{sol,\lambda} \, d\lambda$$

or

$$Q_{abs} = \alpha_1 \int_0^{\lambda_c} G_{sol,\lambda} \, d\lambda + \alpha_2 \int_{\lambda_c}^{\infty} G_{sol,\lambda} \, d\lambda \qquad (2)$$

The assumption implicit here is that the absorptance is independent of the direction of the incoming energy. Surfaces for which this assumption is valid are <u>diffuse</u>. Similarly, the emitted thermal energy may be expressed as the sum of the energies emitted in both bands, i.e.,

$$Q_{emit} = \int_0^{\lambda_c} \varepsilon_\lambda \, e_{b\lambda} \, (T) \, d\lambda + \int_{\lambda_c}^{\infty} \varepsilon_\lambda \, e_{b\lambda} \, d\lambda \qquad (3)$$

where $e_{b\lambda}$ (the spectral emissive power of a black surface) is given by Planck's Law

$$e_{b\lambda}(T) = \frac{2\pi C_1}{\lambda^5 [\exp(C_2/\lambda T)-1]} \quad . \qquad (4)$$

Equation (3) is re-expressed as

$$Q_{emit} = \alpha_1 \int_0^{\lambda_c} e_{b\lambda} \, (T) \, d\lambda + \alpha_2 \int_{\lambda_c}^{\infty} e_{b\lambda} \, (T) \, d\lambda \qquad (5)$$

using the fact that $\varepsilon_\lambda = \alpha_\lambda$ (Kirchoff's Law). Equations (2) and (5), together with the relationships

$F_{sol,\lambda_c} \equiv$ fraction of the solar irradiation at wavelengths less than λ_c

$$= \frac{\int_0^{\lambda_c} G_{sol,\lambda} d\lambda}{\int_0^{\infty} G_{sol,\lambda} d\lambda} , \tag{6}$$

$F_{emit,\lambda_c}(T) \equiv$ fraction of the emissive power of black surface at wavelengths less than λ_c

$$= \frac{\int_0^{\lambda_c} e_{b\lambda}(T) d\lambda}{\int_0^{\infty} e_{b\lambda}(T) d\lambda} , \tag{7}$$

and

$$\int_0^{\infty} e_{b\lambda}(T) d\lambda = \sigma T^4 \tag{8}$$

are substituted into Equation (1) giving the desired expression for absorber efficiency:

$$\boxed{\eta = (\alpha_1 - \alpha_2)\left[F_{sol,\lambda_c} - \frac{\sigma T^4}{G_{sol}} F_{emit,\lambda_c}(T)\right] + \alpha_2 \left(1 - \frac{\sigma T^4}{G_{sol}}\right)} \tag{9}$$

b. Efficiency of a non-selective (gray) surface with the absorptance of band 1 over the entire spectrum

The non-selective surface may be regarded as a selective surface with an infinite cutoff wavelength λ_c. As λ_c becomes infinite, the fractions F_{sol,λ_c} and F_{emit,λ_c} both approach 1 causing Equation (9) to become:

$$\eta_{\substack{\text{non-}\\\text{selective}}} = \alpha_1 \left(1 - \frac{\sigma T^4}{G_{sol}}\right) \tag{10}$$

c. Efficiency in terms of total hemispherical emittance and absorptance

If total hemispherical emittance and absorptance data were available, the emitted and absorbed energies could be calculated from the relationships defining these total properties, i.e.,

$$Q_{emit} = \varepsilon\sigma T^4 \tag{11}$$

and

$$Q_{abs} = \alpha G_{sol} \tag{12}$$

Substituting these expressions into Equation (1) gives

$$\eta = \varepsilon \left(\frac{\alpha}{\varepsilon} - \frac{\sigma T^4}{G_{sol}}\right) \tag{13}$$

It is immediately apparent from the above expression that two surfaces having identical α/ε ratios could have significantly different efficiencies and, therefore, significantly different amounts of net energy input. This is the reason why the efficiency η, and not the α/ε ratio, is used as a measure of absorber performance.

Discussion

Absorber efficiency was computed as a continuous function of λ_c for the two-band model of the spectrally selective absorber using Equation (9). Sample results are given in Figure 3. The fractions F_{sol,λ_c} and F_{emit,λ_c}, required in the computations, were evaluated as described in the Appendix. The salient features of Figure 3 (and other results) are discussed below.

Efficiency is negative if conditions are such that emitted energy exceeds absorbed energy. The efficiency falls as the temperature increases, or the solar irradiation decreases, or both happen. Energy must be supplied to an absorber from external (non-solar) sources if the efficiency is negative.

Efficiency becomes increasingly insensitive to the location of the cutoff as the cutoff wavelength increases as evidenced by the horizontal asymptotes. The reason for this behavior can be deduced from Figures 1 and 2: as the cutoff wavelength passes through the far infrared, leaving the solar and near infrared spectra behind it, the surface begins to assume the behavior of a non-selective surface having the absorptance α_1 over the entire spectrum. Absorber efficiency is, therefore, expressed by Equation (10) for large values of λ_c. For similar reasons, efficiency also becomes insensitive to the position of the cutoff as λ_c approaches 0. In this limit, the efficiency is that of a non-selective surface having the absorptance α_2 over the entire spectrum

$$\lim_{\lambda_c \to 0} \eta = \alpha_2 \left(1 - \frac{\sigma T^4}{G_{sol}}\right)$$

Clearly, however, the most outstanding features of Figure 3 are the maxima in the efficiency curves. For a given set of parameters, T, G_{sol}, α_1 and α_2, efficiency has a maximum at the cutoff wavelength satisfying the condition

$$\frac{\partial \eta}{\partial \lambda_c} = 0 \qquad (14)$$

where η is expressed by Equation (9). The details of the solution of Equation (14) are given in the Appendix for the case of optical air mass 0.

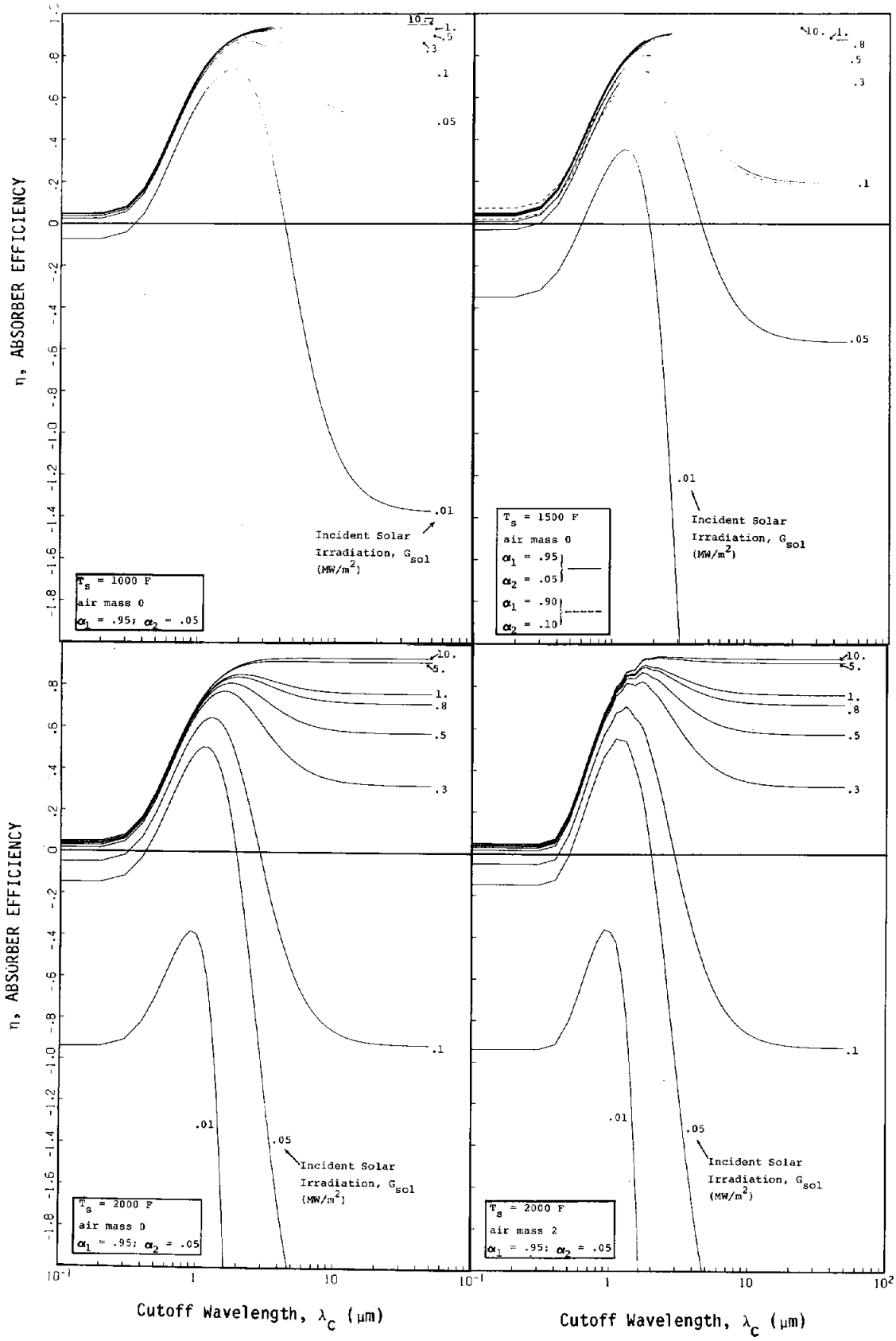

Figure 3. Efficiency of two-band spectrally selective surface as a function of cutoff wavelength λ_c. Note that, as $\lambda_c \to \infty$, the efficiency is that of a non-selective (gray) surface with the absorptance α_1.

The final result is that $\lambda_{c,max}$, the cutoff wavelength which maximizes efficiency, is the solution of the equation

$$\frac{G_{sol}}{\sigma T^4}\left(\frac{T}{T_{sol}}\right)^4 = \frac{\exp(C_2/\lambda_{c,max}T_{sol})-1}{\exp(C_2/\lambda_{c,max}T)-1} \tag{15}$$

It is noteworthy that this equation, and, therefore, $\lambda_{c,max}$, is independent of the band absorptances α_1 and α_2. Equation (15) requires a numerical solution, and sample results are given in Table 1.

Table 1. $\lambda_{c,max}$ Cutoff wavelength which maximizes absorber efficiency (μm)
(Based on optical air mass 0)

G_{sol}, Solar Irradiation (MW/m^2)	T_s, Absorber Surface Temperature (°F)			
	1000.	1500.	2000.	2500.
0.01	1.8	1.2	0.9	0.7
0.05	2.2	1.5	1.1	0.9
0.10	2.5	1.7	1.3	1.0
0.30	3.2	2.1	1.6	1.2
0.50	3.6	2.4	1.7	1.3
0.80	4.2	2.7	2.0	1.5
1.00	4.5	2.9	2.1	1.6
5.00	13.5	6.9	4.3	3.0
10.00	>50	24.0	9.7	5.6

As an illustration of the improvement in efficiency attainable by using a spectrally selective absorber consider the example

absorber temperature	T_s = 1000F
absorptance band 1	α_1 = 0.95
absorptance band 2	α_2 = 0.05
solar irradiation	G_{sol} = 0.10 MW/m^2

The curve in Figure 3 corresponding to these conditions shows that a non-selective surface having the absorptance 0.95 over the entire spectrum has the efficiency $\eta_{\text{non-selective}} = 0.72$, whereas a selective surface with the optimum cutoff wavelength (2.5 μm) has the efficiency $\eta_{max} = 0.89$. (Note that these efficiencies correspond, respectively, to the long-wavelength and peak values of the particular efficiency curve.) The potential improvement in efficiency may be expressed as

$$I = \frac{\eta_{max} - \eta_{\text{non-selective}}}{\eta_{\text{non-selective}}} \tag{16}$$

which, in this example, is

$$I = \frac{0.89 - 0.72}{0.72} = 24\%$$

By examining the other curves in Figure 3, it is evident that greater improvements in efficiency are possible as the surface temperature increases, or the irradiation decreases, or both changes occur. The dependency of the potential improvement in efficiency on irradiation and surface temperature is indicated in Figure 4.[1] At each temperature level, the irradiations corresponding to fixed improvements in efficiency, I, are given on the ordinate. For instance, for an absorber temperature of 1100F, the improvement in efficiency attainable by using a spectrally selective surface could be greater than 50% if the irradiation were less than ~0.085 MW/m^2; whereas the improvement in efficiency would be less than 10% if the irradiation exceeded ~0.25 MW/m^2. The 10% and 50% curves in Figure 4 were fit, respectively, by the following expressions:

---

[1]The data for Figure 4 were calculated by the procedure outlined in the Appendix.

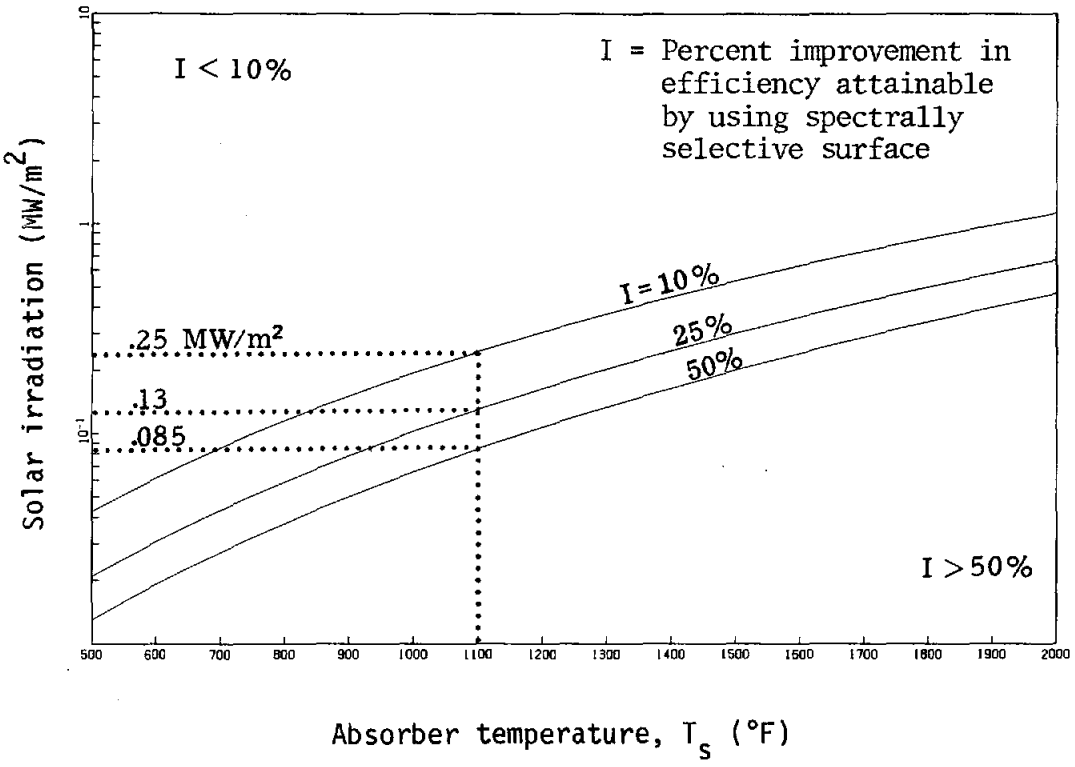

Figure 4. The improvement in efficiency attainable by using a spectrally selective surface instead of a non-selective one. Assumes band 1 and 2 absorptances are, respectively, 1 and 0; also assumes air mass 0 solar irradiation.

$$G_{sol} = 6.783 \times 10^{-3} \exp\left[T_s(-7.586 \times 10^{-7} T_s + 4.073 \times 10^{-3})\right]$$

solar irradiation [MW/m^2] above which the improvement in efficiency would be less than 10%
(T_s absorber temperature in degrees F)

$$G_{sol} = 1.824 \times 10^{-3} \exp\left[T_s(-7.716 \times 10^{-7} T_s + 4.314 \times 10^{-3})\right]$$

solar irradiation [MW/m^2] beneath which the improvement in efficiency could be greater than 50%
(T_s absorber temperature in degrees F)

The bottom two panels in Figure 3 are based on identical conditions except for the optical air masses. Qualitatively, at least, the two sets of results are in agreement, and therefore, efficiency predictions based upon air mass 0 solar irradiation are deemed realistic. Close agreement is not unexpected in view of the similarity of the fractions F_{sol,λ_c} for air masses 0 and 2. (See Figure A1, page 26.) Agreement improves as absorber temperature increases and solar irradiation decreases. The reason is that, as these changes occur, the only air mass-dependent term in Equation (9), F_{sol,λ_c}, becomes less significant.

The sensitivity of efficiency to the band 1 and 2 absorptances is quantified by the derivatives $\partial\eta/\partial\alpha_1$ and $-\partial\eta/\partial\alpha_2$ which can be expressed as

$$\frac{\partial\eta}{\partial\alpha_1} = \left[F_{sol,\lambda_c} - \frac{\sigma T^4}{G_{sol}} F_{emit,\lambda_c}(T)\right] \equiv \frac{\text{Increment in efficiency}}{\text{Increment in band 1 absorptance}} \qquad (18)$$

and

$$\frac{-\partial\eta}{\partial\alpha_2} = \left[F_{sol,\lambda_c} + \frac{\sigma T^4}{G_{sol}} \left(1 - F_{emit,\lambda_c}(T)\right)\right] - 1 \equiv \frac{\text{Increment in efficiency}}{\text{Decrement in band 2 absorptance}} \qquad (19)$$

by differentiating Equation (9). These derivatives are plotted in Figure 5 as a continuous function of absorber temperature for selected values of G_{sol}. The cutoff wavelength corresponding to each plotted point is that which maximizes absorber efficiency. Apart from the self-evident result that increasing α_1 and/or decreasing α_2 improves efficiency, it is apparent that

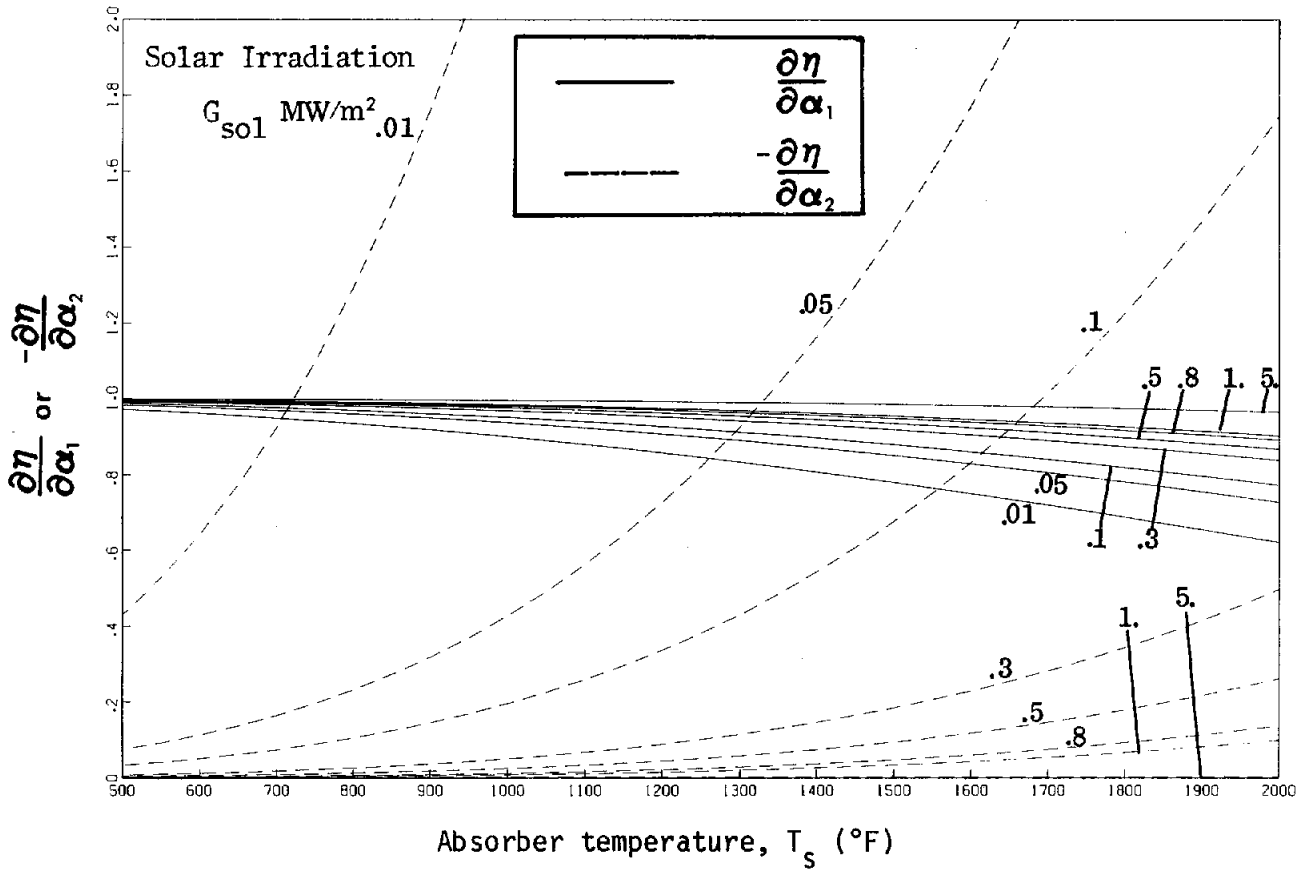

Figure 5. The sensitivity of efficiency to changes in the band 1 and 2 absorptances. Assumes that the transition from band 1 to 2 occurs at the optimum wavelength; also assumes air mass 0 solar irradiation.

α_2 can have a dominant effect upon efficiency for low values of irradiation and high values of temperature. By comparing Equations (17) and (18) it is found that $-\partial\eta/\partial\alpha_2$ exceeds $\partial\eta/\partial\alpha_1$ (and, therefore, reductions in α_2 are more effective than increases in α_1) when $\sigma T^4/G_{sol} > 1$.

Conclusions

Two parameters govern whether a selective surface could be beneficial in a given application: the surface temperature, and the magnitude of the solar irradiation. It becomes increasingly advantageous to use a selective surface (instead of a non-selective, or gray surface) as the temperature increases, or the irradiation decreases, or both happen. The amount of improvement that could be achieved by using a selective surface is quantified in Figure 4.

The cutoff wavelength which maximizes the efficiency of the selective absorber also depends on the surface temperature and solar irradiation. (See Table 1, page 16.) The penalty incurred by not having the cutoff at the optimum value increases as the temperature increases and/or the irradiation decreases. Note that the efficiency curves (Figure 3) become more sharply peaked at the optimum wavelength as these changes occur.

The efficiency depends more on the band 1 absorptance than the band 2 absorptance for conditions of low temperature and high solar irradiation. However, the opposite is true for conditions of high temperature and low solar irradiation. The sensitivity of efficiency to changes in the band 1 and 2 absorptances is quantified in Figure 5.

Finally, it must be recognized that these conclusions are applicable only to exposed absorber surfaces which "see" the solar spectrum. Absorber surfaces which comprise the walls of a cavity may receive a significant amount of infrared energy emitted from elsewhere within the cavity. A detailed study of the radiation heat transfer accounting for the spectral dependence of the radiant energy would be necessary to determine the benefits of spectrally selective surfaces in cavities.

APPENDIX

A. Evaluation of the fractions $F_{emit,\lambda_c}(T)$ and F_{sol,λ_c}

$F_{emit,\lambda_c}(T)$ -- fraction of emissive power of black surface at wavelengths less than λ_c

The analysis outlined below is from a current investigation of cavity-type solar absorbers being conducted at Sandia Laboratories.

From its definition, Equation (7),

$$F_{emit,\lambda_c}(T) = \frac{\int_0^{\lambda_c} e_{b\lambda}(T)\,d\lambda}{\int_0^{\infty} e_{b\lambda}(T)\,d\lambda} \quad . \tag{A1}$$

Substituting Equations (4) and (8) gives

$$F_{emit,\lambda_c}(T) = \frac{2\pi C_1}{\sigma T^4} \int_0^{\lambda_c} \frac{d\lambda}{\lambda^5[\exp(C_2/\lambda T)-1]} \tag{A2}$$

which becomes

$$F_{emit,\lambda_c}(T) = \frac{15}{\pi^4} \int_{C_2/\lambda_c T}^{\infty} \frac{z^3 dz}{e^z-1} \tag{A3}$$

by making the variable substitution

$$z = C_2/\lambda_c T \quad , \tag{A4}$$

and using the fact that the Stefan-Boltzmann constant and the Planck constants C_1 and C_2 are related by

$$\sigma = \frac{2\pi^5 C_1}{15 C_2^4} \quad . \tag{A5}$$

Equation (A5) can be found in Reference 2, page 25.

The indefinite integral in Equation (A3), known as a Debye function, has the series representation [5, page 998]

$$\int_x^\infty \frac{z^3 dx}{e^z - 1} = \sum_{k=1}^{\infty} e^{-kx} \left(\frac{x^3}{k} + \frac{3x^2}{k^2} + \frac{6x}{k^3} + \frac{6}{k^4} \right) \tag{A6}$$

[used in Equation (A3) for $x > 2$]

where $x \equiv C_2/\lambda_c T$. This series converges to the integral for all $x > 0$. However, for $x < 2$, convergence was found to be very slow, and therefore, an alternate means of calculating $F_{emit,\lambda_c}(T)$ was employed in this range. Equation (A3) was first re-expressed as

$$F_{emit,\lambda_c}(T) = \frac{15}{\pi^4} \left[\int_0^\infty \frac{z^3 dz}{e^z - 1} - \int_0^x \frac{z^3 dz}{e^z - 1} \right], \tag{A7}$$

and then the definite integral was replaced by its numerical equivalent, $\pi^4/15$, giving

$$F_{emit,\lambda_c}(T) = 1 - \frac{15}{\pi^4} \int_0^x \frac{z^3 dz}{e^z - 1} \quad . \tag{A8}$$

The above integral, also termed a Debye function, has the series representation [5, page 998]

$$\int_0^x \frac{z^3 dz}{e^z - 1} = x^3 \left[\frac{1}{3} - \frac{x}{8} + \sum_{k=1}^{\infty} \frac{B_{2k} x^{2k}}{(2k+3)(2k)!} \right] \tag{A9}$$

[used in Equation (A8) for $x < 2$]

where B_{2k} is the Bernoulli number of 2k-th order. No convergence difficulties were encountered with this series for $x < 2$.

A FORTRAN subroutine including both series was written and used to evaluate $F_{emit,\lambda_c}(T)$.

F_{sol,λ_c} -- the fraction of the solar irradiation at wavelengths less than λ_c

This fraction is defined in Equation (6) as

$$F_{sol,\lambda_c} = \frac{\int_0^{\lambda_c} G_{sol,\lambda} d\lambda}{\int_0^{\infty} G_{sol,\lambda} d\lambda} \qquad \text{(A10)}$$

For the case of optical air mass 2, F_{sol,λ_c} was calculated as a function of λ_c by integrating Moon's data [6, page 16-9] numerically using the method of overlapping parabolas [7]. The Moon data correspond to an exo-atmospheric irradiation of 1322 watts/m^2 and a sea level irradiation of 741 watts/m^2.

For the case of optical air mass 0, F_{sol,λ_c} was calculated assuming the spectral solar irradiation is a constant multiple of the spectral emissive power of a 5900°K black body. This temperature level best characterizes solar irradiation at the brightest part of the spectrum -- ~5600 Å [6, page 16-1]. Thus,

$$F_{sol,\lambda_c} = F_{emit,\lambda_c} \ (5900°K) \quad \text{[for air mass 0 only]} \qquad \text{(A11)}$$

The fraction F_{sol,λ_c} is plotted in Figure A1 for air masses 0 and 2.

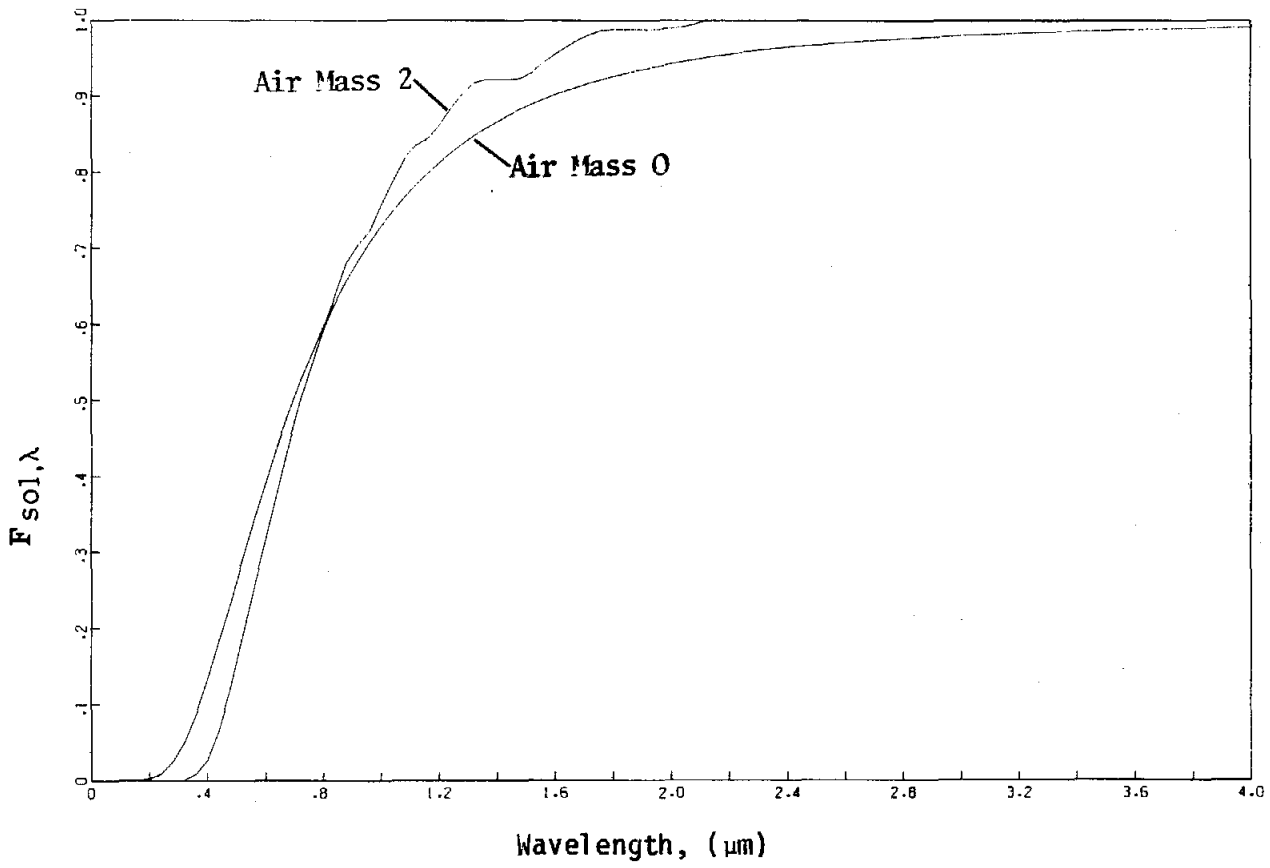

Figure A1. The fraction $F_{sol,\lambda}$ versus wavelength for air masses 0 and 2

B. Determination of the cutoff wavelength which maximizes absorber efficiency

The starting point in this development is Equation (9) which is repeated here for convenience

$$\eta = (\alpha_1-\alpha_2)\left[F_{sol,\lambda_c} - \frac{\sigma T^4}{G_{sol}} F_{emit,\lambda_c}(T)\right] + \alpha_2 \left(1 - \frac{\sigma T^4}{G_{sol}}\right) \qquad (A12)$$

Assuming that the parameters T, G_{sol}, α_1, and α_2 are fixed, we seek the value of λ_c which maximizes the efficiency, η. The optimum λ_c must, therefore, satisfy the equation

$$\frac{\partial \eta}{\partial \lambda_c} = 0 \qquad (A13)$$

or, by substituting Equation (A12),

$$\frac{\partial F_{sol,\lambda_c}}{\partial \lambda_c} - \frac{\sigma T^4}{G_{sol}} \frac{\partial F_{emit,\lambda_c}(T)}{\partial \lambda_c} = 0 \qquad (A14)$$

By differentiating the expression for $F_{emit,\lambda_c}(T)$ [Equation (A3)], it can be shown that

$$\frac{\partial F_{emit,\lambda_c}(T)}{\partial \lambda_c} = \frac{15}{\pi^4} \frac{1}{\lambda_c} \left[\frac{C_2}{\lambda_c T}\right]^4 \Big/ \left[\exp(C_2/\lambda_c T)-1\right] \quad . \qquad (A15)$$

A similar expression for $\partial F_{sol,\lambda_c}/\partial \lambda_c$ results if it is assumed that the spectral solar irradiation corresponds to an optical air mass of 0. In this case Equation (A11) is applicable and

$$\frac{\partial F_{sol,\lambda_c}}{\partial \lambda_c} = \frac{\partial}{\partial \lambda_c} F_{emit,\lambda_c}(T_{sol}) = \frac{15}{\pi^4} \frac{1}{\lambda_c} \left[\frac{C_2}{\lambda_c T_{sol}}\right]^4 \Big/ \left[\exp(C_2/\lambda_c T_{sol})-1\right] \qquad (A16)$$

where T_{sol} = 5900°K. Substituting Equations (A15) and (A16) into (A14), and simplifying the result yields

$$\frac{G_{sol}}{\sigma T^4}\left(\frac{T}{T_{sol}}\right)^4 = \frac{\exp(C_2/\lambda_c T_{sol})-1}{\exp(C_2/\lambda_c T)-1} \quad . \tag{A17}$$

The value of λ_c which satisfies this equation maximizes the expression for absorber efficiency. It is noteworthy that the solution is independent of the band absorptances α_1 and α_2. Different values of λ_c would be obtained for other optical air masses. However, these values would also be independent of α_1 and α_2.

C. The procedure used to calculate the data of Figure 4

The ordinates in Figure 4 were calculated by the following procedure. For each pair of the parameters I and T_s:

a) a trial value of the irradiation G_{sol} was selected;

b) the optimum cutoff wavelength $\lambda_{c,max}$ corresponding to G_{sol} and T_s was then calculated by the numerical solution of Equation (15);

c) η_{max} was calculated by Equation (9) using the foregoing values of $\lambda_{c,max}$, G_{sol}, and T_s;

d) $\eta_{non-selective}$ was calculated by Equation (10);

e) η_{max} and $\eta_{non-selective}$ were substituted into Equation (16) and the resultant value of I was compared to the value of I specified at the outset;

f) the solution procedure was stopped if the two values of I were in agreement, otherwise the procedure was repeated with a new trial value of G_{sol}.

REFERENCES

1. McDonnell-Douglas Preliminary Design Report, Volume 4 - Receiver Subsystem, Report No. MDC G6776, May 1977.

2. Peterson, R. E., and Ramsey, J. W., "Thin Film Coatings in Solar-thermal Power Systems," J. Vac. Sci. Technol., 12, No. 1, pp. 174-181, 1975.

3. Pettit, R. B., and Sowell, R. R., "Solar Absorptance and Emittance of Several Solar Coatings," J. Vac. Sci. Technol., 13, No. 2, pp. 596-602, 1976.

4. Siegel, R., and Howell, J. R., Thermal Radiation Heat Transfer, McGraw-Hill Book Co., New York, 1972.

5. Abramowitz, M., and Stegun, I., Handbook of Mathematical Functions, Dover Publications, Inc., New York, 1965.

6. Valley, S. L., Editor, Handbook of Geophysics and Space Environments, McGraw-Hill Book Co., New York, 1965.

7. Jefferson, T. H., User's Guide to the Sandia Mathematical Program Library at Livermore, Sandia Report No. SAND77-8274, October 1977.

DISTRIBUTION:

Boeing Engineering and Construction
P. O. Box 3707
Seattle, WA 98214
Attn: D. Cox

Solar Energy Division
Department of Energy
San Francisco Operations Office
1333 Broadway
Oakland, CA 94612
Attn: D. Elliot
Attn: M. Schanfein

General Electric Company
Energy Systems and Technology Division
310 De Guigne Drive
Sunnyvale, CA 94086

General Electric Company
Research and Development Center
P. O. Box 43
Schenectady, NY 12301
Attn: G. Fox

Jet Propulsion Laboratory
4800 Oak Grove Drive
Pasadena, CA 91103
Attn: M. A. Adams

Martin Marietta Aerospace Corp.
P. O. Box 179
Denver, CO 80201
Attn: T. Tracy
Attn: D. Gorman

McDonnell-Douglas Corporation
5301 Bolsa Avenue
Huntington Beach, CA 92647
Attn: J. Coleman
Attn: R. W. Hallet

Monsanto Research Corporation
Mound Laboratory
P. O. Box 32
Miamisburg, Ohio 45342
Attn: L. Wittenberg

Rocketdyne, Division of Rockwell International
6633 Canoga Avenue
Canoga Park, CA 91304
Attn: J. M. Friefeld

Atomics International Division
Rockwell International
8900 DeSoto Avenue
Canoga Park, CA 91304
Attn: T. Springer

Solar Energy Research Institute
1536 Cole Boulevard
Golden, CO 80401
Attn: Dr. Barry Butler (1)
P. Call (5)

Dr. R. Viskanta
School of Mechanical Engineering
Purdue University
West Lafayette, IN 47907

Dr. R. Greif
Dept. of Mechanical Engineering
University of California, Berkeley
Berkeley, CA 94720

K. J. Touryan, 1260; Attn: D. F. McVey, 1261
H. C. Hardee, 1262
J. H. Scott, 5700; Attn: G. E. Brandvold, 5710
R. S. Claassen, 5800; Attn: H. J. Saxton, 5840
J. N. Sweet, 5842
M. J. Davis, 5830; Attn: D. M. Mattox, 5834
R. B. Pettit, 5842
T. B. Cook, Jr., 8000; Attn: C. H. DeSelm, 8200
B. F. Murphey, 8300
W. C. Scrivner, 8400
L. Gutierrez, 8100; Attn: D. E. Gregson, 8150
R. D. Cozine, 8160
C. S. Selvage, 8180
W. E. Alzheimer, 8120; Attn: A. L. Jones, 8121
C. S. Hoyle, 8122
W. Zinke, 8123
M. Abrams, 8124 (5)
A. F. Baker, 8124
R. C. Wayne, 8130
W. G. Wilson, 8131
A. C. Skinrood, 8132 (15)
E. T. Cull, 8132
L. A. Hiles, 8132
L. G. Radosevich, 8132
L. N. Tallerico, 8132
G. W. Anderson, 8140; Attn: A. R. Willis, 8144
D. M. Schuster, 8310; Attn: W. R. Hoover, 8314
P. J. Eicker, 8326; Attn: J. B. Woodard
Technical Publications and Public Information Division, 8265, for TIC (2)
F. J. Cupps, 8265/Technical Library Processes Division, 3141
Technical Library Processes Division, 3141 (2)
Library and Security Classification Division, 8266-2 (3)